



PCCP

**Temperature and Solvent-Dependent Photoluminescence
Quenching in [Ru(bpy)₂(bpy-cc-AQ)]²⁺**

Journal:	<i>Physical Chemistry Chemical Physics</i>
Manuscript ID	CP-ART-09-2020-005044.R1
Article Type:	Paper
Date Submitted by the Author:	11-Dec-2020
Complete List of Authors:	Larsen, Christopher; SLAC,

SCHOLARONE™
Manuscripts

ARTICLE

Temperature and Solvent-Dependent Photoluminescence Quenching in $[\text{Ru}(\text{bpy})_2(\text{bpy-cc-AQ})]^{2+}$

Christopher B. Larsen^{*a}

Received 00th January 20xx,
Accepted 00th January 20xx

DOI: 10.1039/x0xx00000x

I have herein investigated the solvent-dependent photoluminescence quenching mechanism of $[\text{Ru}(\text{bpy})_2(\text{bpy-cc-AQ})]^{2+}$ using variable temperature emission spectroscopies. The photophysics of this complex are dominated by an excited-state thermal equilibrium between a photoluminescent $^3\text{MLCT}$ state and a charge-separated state that lies higher in energy relative to the $^3\text{MLCT}$ state in low polarity solvents and approximately isoenergetic in high polarity solvents. Furthermore, an unusual photoluminescence temperature-dependence in high polarity solvents is shown to arise from competition between enthalpic factors favouring the charge-separated state and entropic factors favouring the photoluminescent $^3\text{MLCT}$ state, analogous to the molecular light-switch effect of $[\text{Ru}(\text{bpy})_2(\text{dppz})]^{2+}$. The solvent-dependent photoluminescence quenching of $[\text{Ru}(\text{bpy})_2(\text{bpy-cc-AQ})]^{2+}$ is attributed to two key solvent-dependent factors: (1) the excited-state equilibrium position and (2) the rate of charge-recombination from the charge-separated state.

Introduction

The development of molecular systems in which photoluminescence can be switched on/off upon interaction with an external stimulus provides the foundation for both molecular logic and sensing applications.¹⁻¹⁷ Whilst photoluminescence modulation upon binding of chemical analytes¹⁻¹² and through photochromic transformations is well-established,¹³⁻¹⁷ the use of solvent and temperature are significantly less explored.

The potential of solvent to modulate photoluminescence is well-demonstrated by the molecular light-switch effect of $[\text{Ru}(\text{bpy})_2(\text{dppz})]^{2+}$ (Figure 1 left, bpy = 2,2'-bipyridine, dppz = dipyrido[3,2- α :2',3'- c]phenazine) and related complexes, in which the complex exhibits bright photoluminescence in aprotic solvents or when intercalated into double-strand DNA, but is non-luminescent in protic solvents/aqueous media.^{18, 19} It has long been known that this phenomenon arises from two closely-lying acceptor orbitals localised on the bipyridine and phenazine sections of the dppz ligand, which in combination with the metal, form a photoluminescent $^3\text{MLCT}$ excited state and a non-luminescent charge-separated (CS) state, respectively.²⁰⁻³²

In two key studies, Brennaman *et al.* demonstrated that the molecular light-switch effect of $[\text{Ru}(\text{bpy})_2(\text{dppz})]^{2+}$ arises from an excited-state thermal equilibrium between these two states, wherein the CS state is always enthalpically favoured (at least over the investigated solvent range) and the $^3\text{MLCT}$ state entropically favoured, which was attributed to the separation

of charge inducing greater order in the surrounding solvent.^{33, 34} The competition between enthalpic and entropic factors results in an unusual inversion of excited-state populations, such that the photoluminescent $^3\text{MLCT}$ state dominates in aprotic solvents (or in the presence of double-strand DNA), and the CS state in protic solvents, which gives rise to the large environment-dependent contrast from which the effect derives its name.

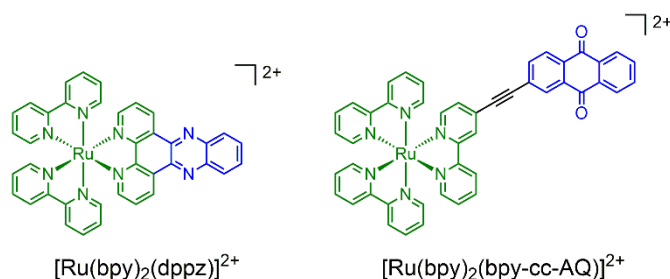


Figure 1. Chemical structures of $[\text{Ru}(\text{bpy})_2(\text{dppz})]^{2+}$ (left) and $[\text{Ru}(\text{bpy})_2(\text{bpy-cc-AQ})]^{2+}$ (right). Green sections represent $[\text{Ru}(\text{bpy})_2]^{2+}$ photosensitiser core, blue sections represent electron acceptors that contribute to the respective CS states.

The utility of excited-state thermal equilibria in modulating photophysical properties has also been demonstrated within the contexts of excited-state deactivation through ligand-field channels,^{35, 36} thermally-activated delayed fluorescence (TADF) for OLED applications,³⁷⁻³⁹ and photoluminescence lifetime elongation through the 'triplet reservoir' effect.⁴⁰⁻⁴²

Within the context of developing new systems in which solvent could modulate photoluminescence properties through activation/deactivation of intramolecular electron-transfer (ET), myself and others recently reported a molecular dyad comprised of a $[\text{Ru}(\text{bpy})_3]^{2+}$ photosensitiser and an anthraquinone (AQ) acceptor coupled by an ethynyl (cc) linker ($[\text{Ru}(\text{bpy})_2(\text{bpy-cc-AQ})]^{2+}$, Figure 1 right).⁴³ We demonstrated

^aStanford PULSE Institute, SLAC National Accelerator Laboratory, Stanford University, 2575 Sand Hill Road, Menlo Park, CA 94025, USA

[†]Electronic Supplementary Information (ESI) available: Variable Temperature Photoluminescence Lifetime Fitting, Marcus Theory Considerations, and Dielectric Continuum Model Solvent Effects. See DOI: 10.1039/x0xx00000x

that the photoluminescence quantum yield and lifetime of $[\text{Ru}(\text{bpy})_2(\text{bpy-cc-AQ})]^{2+}$ could be modulated over several orders of magnitude as a function of solvent dielectric constant and hydrogen-bond donor strength. This was assigned to solvent-mediated activation/deactivation of ET from a photoluminescent $^3\text{MLCT}$ excited-state to the AQ acceptor, and ultrafast optical transient absorption and time-resolved infrared spectroscopies provided direct evidence for formation of the resultant CS state and for rapid formation of an excited-state thermal equilibrium/pseudoequilibrium.

I herein investigate the mechanism of solvent-dependent photoluminescence quenching of $[\text{Ru}(\text{bpy})_2(\text{bpy-cc-AQ})]^{2+}$ in greater detail using variable temperature emission spectroscopies. I observe an unusual temperature-dependence of photoluminescence intensities and lifetimes in high polarity solvents, attributed to an excited-state thermal equilibrium highly reminiscent of that observed for $[\text{Ru}(\text{bpy})_2(\text{dppz})]^{2+}$, driven by competing enthalpic and entropic factors favouring the CS and $^3\text{MLCT}$ states, respectively. The solvent-dependent photoluminescence quenching of $[\text{Ru}(\text{bpy})_2(\text{bpy-cc-AQ})]^{2+}$ is attributed to two key solvent-dependent factors: (1) the excited-state equilibrium position and (2) the rate of charge-recombination from the CS state.

Results and Discussion

Variable temperature photoluminescence spectra, decay traces and corresponding lifetimes upon excitation into the MLCT absorption manifold (see ref. 43 for absorption spectra) of $[\text{Ru}(\text{bpy})_2(\text{bpy-cc-AQ})]^{2+}$ in 1,2-dichloroethane ($\epsilon = 10.4$), butyronitrile ($\epsilon = 20.7$), acetonitrile ($\epsilon = 36.6$) and ethanol ($\epsilon = 24.6$) are presented in Figure 2. Photoluminescence decays are monoexponential in all solvents and at all recorded temperatures.

In 1,2-dichloroethane, the photoluminescence intensity decreases with increasing temperature, and the photoluminescence lifetime concomitantly decreases, whereas the opposite trend is observed in the higher polarity solvents. The simplest explanation for this behaviour is a reversal in excited-state ordering, whereby the CS state lies higher in energy relative to the $^3\text{MLCT}$ state in low polarity solvents, and lower in high polarity solvents (Figure 3), such that the $^3\text{MLCT}$ state thermally repopulates.

Myself and others have previously demonstrated that transient absorption spectra of $[\text{Ru}(\text{bpy})_2(\text{bpy-cc-AQ})]^{2+}$ are dominated by signals associated with the $^3\text{MLCT}$ state, even in high polarity solvents, and exhibit identical kinetics to the respective photoluminescence decays.⁴³ Previous works have attributed similar behaviour to the rate of charge-recombination (k_{CR}) being greater than the rate of charge-separation (k_{ET} in Figure 3), such that the CS state does not accumulate sufficiently to be experimentally observed.^{44, 45} However, this explanation fails to account for the thermal repopulation of the $^3\text{MLCT}$ state observed in the higher polarity solvents, as it would necessarily require the rate of endergonic back electron-transfer (k_{BET} in Figure 3) to be greater than exergonic k_{ET} . Ultrafast spectroscopies provided direct evidence for rapid

establishment of an excited-state thermal equilibrium/pseudo-equilibrium,⁴³ which is more consistent with the observed variable-temperature photoluminescence behaviour.

For a thermally equilibrated excited-state manifold, depopulation of the excited-state manifold to the ground-state is described by the sum of the decay rates of all individual states (k_i) weighted by their equilibrium populations (n_i) in Equation 1, where N is the total excited-state population at a given point in time (t) and k_{obs} the observed rate constant (defined as the inverse of the observed lifetime, τ_{obs}).⁴⁶

$$\frac{\partial N}{\partial t} = -N \cdot k_{\text{obs}} = -\sum_{i=1} k_i n_i \quad (1)$$

n_i is further expressed as a Boltzmann distribution in Equation 2, where G_i is the free energy of a given state and k_B the Boltzmann constant (8.617×10^{-5} eV K⁻¹).

$$n_i = \frac{N \cdot e^{\left(\frac{-G_i}{k_B T}\right)}}{\sum_{j=1} e^{\left(\frac{-G_j}{k_B T}\right)}} \quad (2)$$

Working with this thermally equilibrated two-state model as depicted in Figure 3, Equation 3 is derived from Equations 1 and 2, where k_{MLCT} is the rate of depopulation of the $^3\text{MLCT}$ excited-state to the ground-state (combining both radiative and non-radiative channels), k_{CR} the rate of charge-recombination (i.e. depopulation from the CS state to the ground-state), and ΔG_{ET} the reaction free energy for ET. This derivation can be found in the supporting information of ref. 43.

$$k_{\text{obs}} = \frac{k_{\text{MLCT}} + k_{\text{CR}} \cdot e^{\left(\frac{-\Delta G_{\text{ET}}}{k_B T}\right)}}{1 + e^{\left(\frac{-\Delta G_{\text{ET}}}{k_B T}\right)}} \quad (3)$$

Equation 3 satisfactorily models the variable temperature behaviour of the photoluminescence lifetimes in 1,2-dichloroethane, from which a ΔG_{ET} of 0.27 eV (2180 cm⁻¹) is obtained (Table 1, top entry). In Equation 3, I have assigned the higher energy (depopulating) state as the CS state, as it is well-established that the ligand-field states lie 3000-3500 cm⁻¹ higher in energy than the $^3\text{MLCT}$ state in $[\text{Ru}(\text{bpy})_3]^{2+}$,^{33-35, 47, 48} and even higher still in analogues with electron-withdrawing substituents or extended conjugation on the ligand,⁴⁹⁻⁵¹ as is the case with $[\text{Ru}(\text{bpy})_2(\text{bpy-cc-AQ})]^{2+}$. However, the possibility of deactivation through the nominally $^3\text{T}_{1g}$ ligand-field state (under the approximation of octahedral geometry) cannot be fully discounted. Indeed, the derived value of τ_{CR} (k_{CR}^{-1}) is more consistent with ligand-field deactivation than what would be expected from Marcus inverted region kinetics (see below). Although there is no direct evidence for multiple deactivating states, as employing an appropriate three-state model does not improve the goodness-of-fit, it is plausible that the ligand-field and CS states are energetically proximal, and the derived value of τ_{CR} represents a population weighted average of the two respective decay rates.

In contrast, Equation 3 is unable to even qualitatively reproduce the variable temperature behaviour of the photoluminescence

lifetimes in the higher polarity solvents. However, the observation of monoexponential photoluminescence decays in all investigated solvents implies that the excited-state manifold is thermally equilibrated, and that the divergence in behaviour arises from the temperature-dependence of ΔG_{ET} . In Equation 4, ΔG_{ET} is therefore expressed as $\Delta H_{ET} - T\Delta S_{ET}$, where ΔH_{ET} and ΔS_{ET} are the reaction enthalpy and entropy, respectively, of ET.

$$k_{obs} = \frac{k_{MLCT} + k_{CR} \cdot e^{-\left(\frac{\Delta H_{ET} - T\Delta S_{ET}}{k_B T}\right)}}{1 + e^{-\left(\frac{\Delta H_{ET} - T\Delta S_{ET}}{k_B T}\right)}} \quad (4)$$

Equation 4 satisfactorily models the variable temperature behaviour of the photoluminescence lifetimes in the high polarity solvents (Figure 2, right). Resultant fit parameters are presented in Table 1. My intent from modelling the variable temperature photoluminescence lifetimes is not to quantitatively assess individual rate constants, but rather to qualitatively explain the unusual observation of increasing photoluminescence lifetimes with increasing temperature. The temperature range is too narrow (see SI, p. S1-2), and the model too simple for quantitative analysis. For example, Equations 3 and 4 do not consider state degeneracies, treating the photoluminescent 3MLCT state as a single state, whereas it is well-established that $[Ru(bpy)_3]^{2+}$ possesses four close-lying $MLCT$ excited states that are thermally equilibrated at temperatures relevant to this work.^{33, 35, 46, 52, 53} Furthermore,

k_{CR} is treated as a temperature-independent term, whereas k_{CR} is dictated by Marcus theory and would therefore be expected to exhibit a temperature-dependence (assuming charge-recombination does not occur in the barrierless region of the Marcus parabola).^{54, 55} It should be noted that a temperature-dependence of k_{CR} alone cannot account for the observed variable temperature photoluminescence lifetime behaviour (see SI, p. S2). It is therefore evident that τ_{obs} is dominated by thermally-induced changes in the equilibrium position rather than in k_{CR} . In principle, this arises because the activation energy for charge-recombination is less sensitive than the excited-state equilibrium constant (K_{eq}) to changes in ΔG_{ET} (see SI, p. S3). The derived values of τ_{CR} in the high polarity solvents (Table 1) imply Marcus inverted region kinetics not too far from the barrierless region, which would further exacerbate this difference in sensitivity. The value derived for 1,2-dichloroethane is an evident outlier, which may be attributed to the influence of ligand-field deactivating states (see above).

As the above considerations negate quantification of individual rate constants, it suffices to note that k_{CR} is substantially greater than k_{MLCT} in all investigated solvents (Table 1), in line with expectation for a strongly-coupled system with a short donor-acceptor distance. It also should be noted that Equations 3 and 4 are only valid if establishment of the excited-state equilibrium ($k_{ET} + k_{BET}$), which has previously been determined to be on the order of a few tens of picoseconds,⁴³ is rapid with respect to k_{MLCT} and k_{CR} .

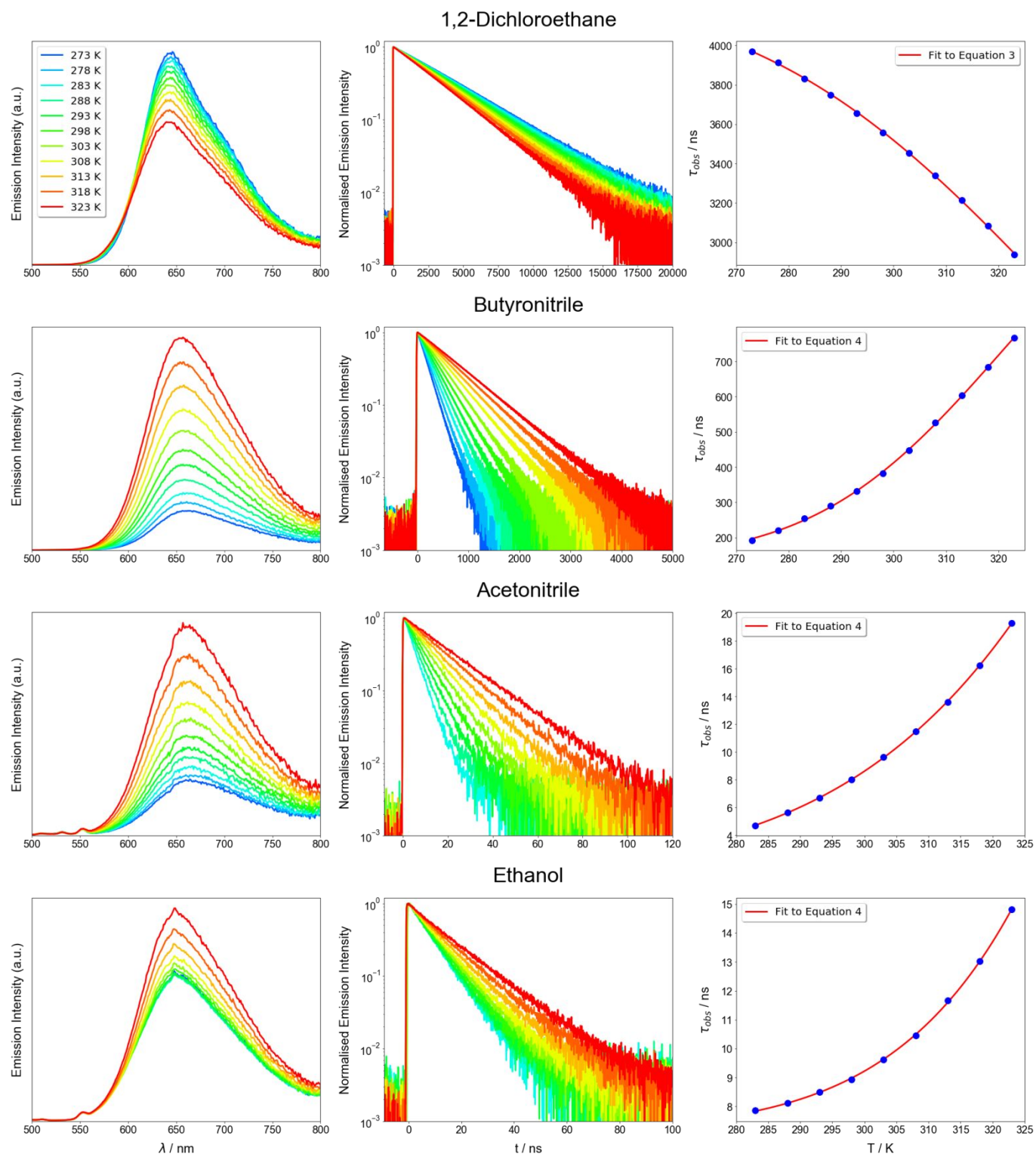


Figure 2. Variable temperature emission spectra (left), decay traces (centre) and corresponding lifetimes (right) of $[\text{Ru}(\text{bpy})_2(\text{bpy-cc-AQ})](\text{PF}_6)_2$ in 1,2-dichloroethane, butyronitrile, acetonitrile and $[\text{Ru}(\text{bpy})_2(\text{bpy-cc-AQ})]\text{Cl}_2$ in ethanol (20 μM , $\lambda_{\text{ex}} = 475 \text{ nm}$). Derived fit parameters are reported in Table 1.

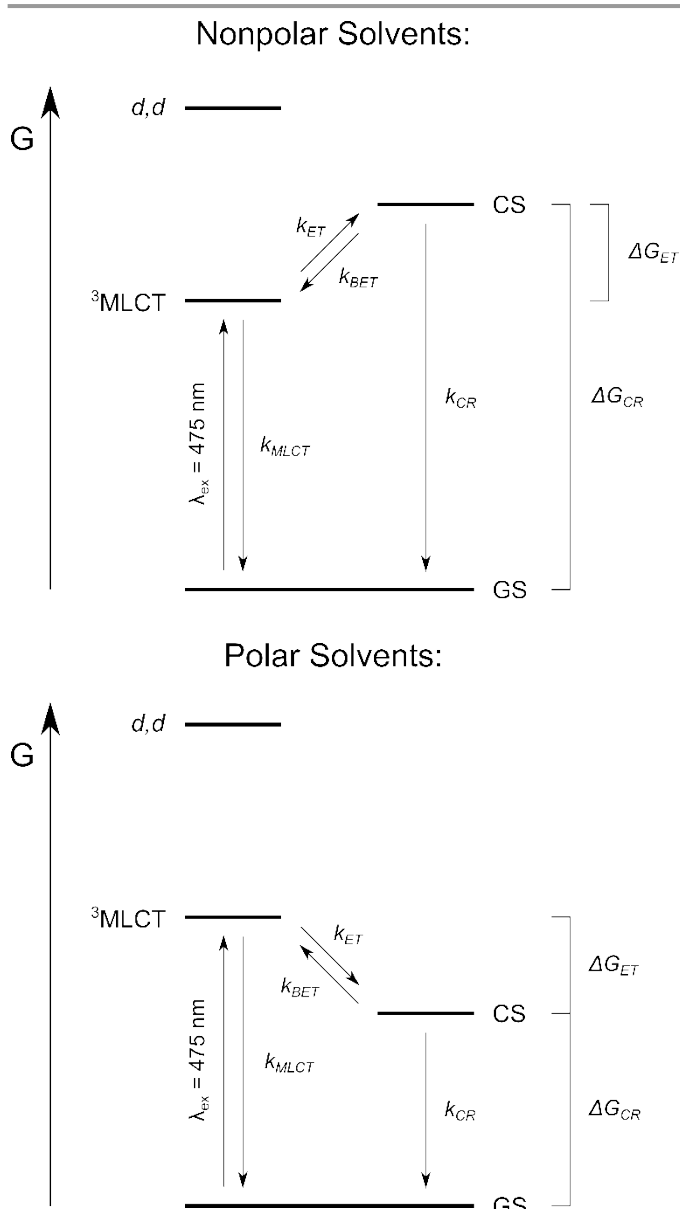


Figure 3. Jablonski diagram depicting excited states of $[\text{Ru}(\text{bpy})_2(\text{bpy-cc-AQ})]^{2+}$ used to construct the kinetic model employed in Equations 3-5. Arrows connecting the d,d states are omitted as they are not explicitly accounted for in Equations 3-5.

Qualitatively, it can be observed that the CS state is enthalpically favoured ($\Delta H_{ET} < 0$) in all solvents except 1,2-dichloroethane, and entropically disfavoured ($\Delta S_{ET} < 0$). A negative ΔS_{ET} indicates greater order associated with the CS state relative to the $^3\text{MLCT}$ state. Analogous to $[\text{Ru}(\text{bpy})_2(\text{dppz})]^{2+}$,^{33, 34} I attribute this observation to the CS state inducing greater order in the surrounding solvent. Similar arguments have also been previously used to explain negative ΔS_{ET} values for electron-transfer reactions and equilibria.⁵⁶⁻⁶¹ The lack of contribution from ΔS_{ET} in 1,2-dichloroethane is likely due to low dielectric constant solvents (with concomitantly small dipole moments) being less sensitive to the change in electronic structure between the $^3\text{MLCT}$ and CS states – i.e. the degree of order in the solvent induced by charge-separation is lesser than for high dielectric constant solvents. Conceptually,

this is analogous to the Lippert-Mataga model for fluorescence solvatochromism.⁶²

Table 1. Parameters derived from least squares fitting of variable-temperature lifetimes of $[\text{Ru}(\text{bpy})_2(\text{bpy-cc-AQ})]^{2+}$ to Equations 3 and 4.

Solvent	$\tau_{\text{MLCT}} / \mu\text{s}$	$\tau_{\text{CR}} / \text{ns}$	$\Delta G_{ET} / \text{eV}$	$\Delta H_{ET} / \text{eV}$	$\Delta S_{ET} / \text{meV K}^{-1}$
1,2-dichloroethane ^a	4.27	0.58	0.27	-	-
Butyronitrile ^b	4.27 ^c	89.2	-	-0.31	-1.15
Acetonitrile ^b	4.27 ^c	1.31	-	-0.33	-1.24
Ethanol ^b	4.27 ^c	7.16	-	-0.48	-1.49

^a Fitted to Equation 3. ^b Fitted to Equation 4. ^c Parameter constrained, see SI p.S1 for details.

Using the parameters derived from fitting of the variable-temperature emission lifetimes with Equations 3 and 4 (Table 1), the excited-state equilibrium constant (K_{eq}), defined as the CS state population (n_{CS}) / the $^3\text{MLCT}$ state population (n_{MLCT}), can be obtained from Equation 5.

$$K_{eq} = \frac{n_{CS}}{n_{\text{MLCT}}} = \frac{k_{ET}}{k_{BET}} = e^{-\left(\frac{\Delta G_{ET}}{k_B T}\right)} = e^{-\left(\frac{\Delta H_{ET} - T \Delta S_{ET}}{k_B T}\right)} \quad (5)$$

The temperature-dependence of K_{eq} in each of the investigated solvents is presented in Figure 4. It can be observed that the CS state is dominant in EtOH, and the photoluminescent $^3\text{MLCT}$ state in all other solvents. For $[\text{Ru}(\text{bpy})_2(\text{dppz})]^{2+}$, such solvent-dependent population inversion was proposed to drive the molecular light-switch effect. An interesting consequence of the competing enthalpic (favouring the CS state) and entropic (favouring the $^3\text{MLCT}$ state) factors in the high polarity solvents is that excited-state equilibrium can also be thermally tuned to invert the relative populations of the two states. Although only limited population inversion occurs over the investigated temperature range, it is evident that judicious solvent selection could in principle result in population inversion at ambient temperatures.

Whilst it may seem counterintuitive that the $^3\text{MLCT}$ state is dominant in butyronitrile and acetonitrile, this observation is consistent with my previous finding that the transient absorption spectra of $[\text{Ru}(\text{bpy})_2(\text{bpy-cc-AQ})]^{2+}$ are dominated by signals associated with a $^3\text{MLCT}$ state in these solvents at room-temperature.⁴³

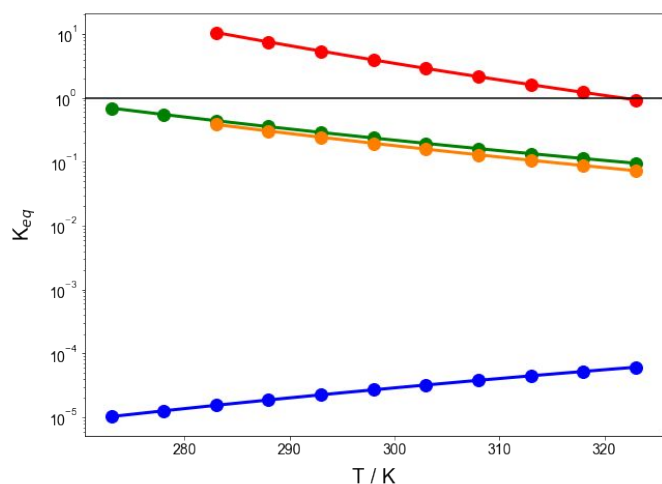


Figure 4. Temperature-dependence of the excited-state equilibrium constant (K_{eq}) of $[\text{Ru}(\text{bpy})_2(\text{bpy-cc-AQ})]^{2+}$ in 1,2-dichloroethane (blue), butyronitrile (green), acetonitrile (orange) and ethanol (red). Black line depicts $K_{eq} = 1$, where $n_{\text{MLCT}} = n_{\text{CS}}$.

Differences in excited-state equilibria appear insufficient to explain the difference in photoluminescence lifetimes between butyronitrile and acetonitrile. Although the fit parameters derived from Equation 4 cannot be quantitatively analysed (see above), it is evident that k_{CR} is significantly greater in acetonitrile than butyronitrile (Table 1), which gives rise to the difference in photoluminescence lifetimes between the two solvents. This can be conceptually understood within the context of Marcus theory: according to the semi-classical Marcus equation (Equation 6),^{54, 55} where λ is the reorganisation energy and H_{DA} the electronic coupling between donor and acceptor, as ΔG_{ET} increases or decreases as a function of solvent polarity, the free energy of charge-recombination, ΔG_{CR} , concomitantly decreases or increases, respectively, which modulates k_{CR} .

$$k_{CR} = \sqrt{\frac{\pi}{h^2 \lambda k_B T}} H_{DA}^2 e^{\left(\frac{-\lambda + \Delta G_{CR}}{4 \lambda k_B T}\right)^2} \quad (6)$$

Employing a dielectric continuum model, the solvent-dependence of ΔG_{CR} can be described using Equation 7,^{63, 64} where ΔG_{vac} is the free energy change in the gas phase, Δe the number of electrons transferred, ϵ_0 the permittivity of free space ($8.854 \times 10^{-12} \text{ C}^2 \text{ N}^{-1} \text{ m}^{-2}$), a_1 and a_2 the spherical radii of the donor and acceptor, respectively, r_{DA} the donor-acceptor distance, and ϵ_s the solvent dielectric constant.

$$-\Delta G_{CR} = \Delta G_{vac} + \frac{\Delta e^2}{4\pi\epsilon_0} \cdot \left(\frac{1}{2a_1} + \frac{1}{2a_2} - \frac{1}{r_{DA}}\right) \left(\frac{1}{\epsilon_s} - 1\right) \quad (7)$$

Furthermore, λ is comprised of an inner-sphere (λ_i) and outer-sphere (λ_o) component (Equation 8), where η_s is the solvent refractive index.⁶³

$$\lambda = \lambda_i + \lambda_o \quad (8a)$$

$$\lambda_o = \frac{\Delta e^2}{4\pi\epsilon_0} \cdot \left(\frac{1}{2a_1} + \frac{1}{2a_2} - \frac{1}{r_{DA}}\right) \left(\frac{1}{\eta_s^2} - \frac{1}{\epsilon_s}\right) \quad (8b)$$

λ_i , a_1 , a_2 and r_{DA} are parameters inherent to a given molecule and are solvent-independent. The effect of increasing ϵ_s is therefore to increase λ . Using donor and acceptor radii (a_1 and a_2) of 4 Å, and r_{DA} of 12.8 Å (estimated from a molecular mechanics model of $[\text{Ru}(\text{bpy})_2(\text{bpy-cc-AQ})]^{2+}$), ΔG_{vac} of 4.57 eV (estimated from electrochemical potentials, see SI, p. S3), and hypothetical values for λ_i of 0 eV and H_{DA} of 21.1 cm^{-1} (2.62 meV), Equations 6-8 yield best fit τ_{CR} values of 89.1 and 2.74 ns in butyronitrile and acetonitrile, respectively. Although this approach is very rough and the derived values above inaccurate, it is evident that the difference in solvent polarity between butyronitrile and acetonitrile can account for such a difference in k_{CR} .

It is, however, also plausible that specific solvation interactions contribute to the difference in k_{CR} between the two solvents. It has already been demonstrated that hydrogen-bonding solvents strongly modulate the photoluminescence lifetimes of $[\text{Ru}(\text{bpy})_2(\text{bpy-cc-AQ})]^{2+}$,⁴³ and Table 1 shows a clear difference in τ_{CR} between butyronitrile and ethanol, which possess similar dielectric constants, but drastically different Reichardt parameters ($E_T^N = 0.364$ and 0.654, respectively),⁶⁵ a known proxy for hydrogen-bond donor strength.^{43, 65-67} For acetonitrile, $E_T^N = 0.460$, indicating the potential for specific solvent-solute interactions to contribute to the difference in τ_{CR} between butyronitrile and acetonitrile.

Whilst globally fitting the photoluminescence decay traces to a specific kinetic model including Marcus parameters could theoretically explain the difference in k_{CR} , the acquired data would require both a larger temperature range and greater temporal resolution for such analysis to be reliable. Such a fit would be further complicated by the fact that, as with ΔG_{ET} , ΔG_{CR} likely shows a temperature-dependence due to charge-recombination being entropically favoured (in contrast to charge-separation being entropically disfavoured).

In any case, these findings clearly demonstrate that the solvent-dependent photoluminescence quenching in $[\text{Ru}(\text{bpy})_2(\text{bpy-cc-AQ})]^{2+}$ arises from a combination of two solvent-dependent factors: the excited-state equilibrium position and the rate of charge-recombination.

Conclusions

I have herein investigated the solvent-dependent photoluminescence quenching mechanism of $[\text{Ru}(\text{bpy})_2(\text{bpy-cc-AQ})]^{2+}$ using variable temperature emission spectroscopies.

The photophysics of this complex are dominated by an excited-state thermal equilibrium between a photoluminescent ³MLCT state and a CS state that lies higher in energy relative to the ³MLCT state in low polarity solvents and approximately isoenergetic in high polarity solvents. Electron-transfer from the $[\text{Ru}(\text{bpy})_3]^{2+}$ photosensitiser to the AQ acceptor is therefore endothermic in low polarity solvents and exothermic in high polarity solvents.

I have demonstrated that an unusual photoluminescence intensity and lifetime temperature-dependence in high polarity solvents arises from competition between enthalpic factors favouring the CS state and entropic factors favouring the ³MLCT

state, which facilitates both solvent- and temperature-dependent population inversion between the two states. This behaviour is reminiscent of the molecular light-switch effect of $[\text{Ru}(\text{bpy})_2(\text{dppz})]^{2+}$.

The high sensitivity of the photoluminescence properties of $[\text{Ru}(\text{bpy})_2(\text{bpy-cc-AQ})]^{2+}$ to solvent polarity can be attributed to two key solvent polarity-dependent factors: (1) the excited-state equilibrium position and (2) the rate of charge-recombination from the CS state.

These results provide greater insight into the solvent-mediated activation/deactivation of photoinduced electron-transfer mechanism that I and others recently reported for $[\text{Ru}(\text{bpy})_2(\text{bpy-cc-AQ})]^{2+}$, and highlight the combined potential of solvent and temperature to elicit large changes in photoluminescence properties – aiding in the development of design principles for solvent- or external field-based molecular switches.

Experimental

The synthesis of $[\text{Ru}(\text{bpy})_2(\text{bpy-cc-AQ})](\text{PF}_6)_2$ and $[\text{Ru}(\text{bpy})_2(\text{bpy-cc-AQ})]\text{Cl}_2$ has already been reported.⁴³ The variable temperature emission spectra and lifetimes of $[\text{Ru}(\text{bpy})_2(\text{bpy-cc-AQ})](\text{PF}_6)_2$ in 1,2-dichloroethane, butyronitrile and acetonitrile have also been reported.⁴³

Variable temperature emission spectra of $[\text{Ru}(\text{bpy})_2(\text{bpy-cc-AQ})]\text{Cl}_2$ in ethanol were recorded as a 20 μM de-aerated solution on a Fluorolog-322 instrument from Horiba Jobin-Yvon equipped with a thermoelectric temperature controller.

Variable emission decay traces of $[\text{Ru}(\text{bpy})_2(\text{bpy-cc-AQ})]\text{Cl}_2$ in ethanol were recorded as a 20 μM de-aerated solution on a Lifespec II time-correlated single photon counting (TCSPC) fluorescence lifetime spectrometer from Edinburgh Instruments, equipped with an EPL-475 pulsed diode laser (Edinburgh Instruments) and a thermoelectric temperature controller.

Data processing and analysis was performed using home-written python scripts. Fitting procedures employed a least-squares approach (trust region reflective algorithm) on the residuals, as implemented in the SciPy library.

Conflicts of interest

There are no conflicts to declare.

Acknowledgements

This work was supported by the U.S. Department of Energy, Office of Science, Basic Energy Sciences, Chemical Sciences, Geosciences, and Biosciences Division. I thank Prof. Kelly Gaffney and Dr Amy Cordones-Hahn for proof-reading this manuscript.

Notes and references

1. J. Andréasson and U. Pischel, *Chem. Soc. Rev.*, 2010, **39**, 174-188.
2. J. Andréasson and U. Pischel, *Chem. Soc. Rev.*, 2015, **44**, 1053-1069.
3. V. Balzani, A. Credi and M. Venturi, *ChemPhysChem*, 2003, **4**, 49-59.
4. A. P. de Silva and N. D. McClenaghan, *Chem. Eur. J.*, 2004, **10**, 574-586.
5. A. P. de Silva and S. Uchiyama, *Nat. Nanotechnol.*, 2007, **2**, 399.
6. B. Daly, J. Ling and A. P. de Silva, *Chem. Soc. Rev.*, 2015, **44**, 4203-4211.
7. A. P. de Silva, D. B. Fox, A. J. M. Huxley and T. S. Moody, *Coord. Chem. Rev.*, 2000, **205**, 41-57.
8. T. Gunnlaugsson, M. Glynn, G. M. Tocci, P. E. Kruger and F. M. Pfeffer, *Coord. Chem. Rev.*, 2006, **250**, 3094-3117.
9. M. H. Keefe, K. D. Benkstein and J. T. Hupp, *Coord. Chem. Rev.*, 2000, **205**, 201-228.
10. Z. Liu, W. He and Z. Guo, *Chem. Soc. Rev.*, 2013, **42**, 1568-1600.
11. B. Valeur and I. Leray, *Coord. Chem. Rev.*, 2000, **205**, 3-40.
12. L. Fabbrizzi and A. Poggi, *Chem. Soc. Rev.*, 1995, **24**, 197-202.
13. G. Copley, T. A. Moore, A. L. Moore and D. Gust, *Adv. Mater.*, 2013, **25**, 456-461.
14. D. Gust, J. Andréasson, U. Pischel, T. A. Moore and A. L. Moore, *Chem. Commun.*, 2012, **48**, 1947-1957.
15. D. Gust, T. A. Moore and A. L. Moore, *Chem. Commun.*, 2006, 1169-1178.
16. F. M. Raymo and M. Tomasulo, *Chem. Soc. Rev.*, 2005, **34**, 327-336.
17. H. Tian and S. Yang, *Chem. Soc. Rev.*, 2004, **33**, 85-97.
18. J.-P. Sauvage and N. J. Turro, *J. Am. Chem. Soc.*, 1990, **11**, 4960-4962.
19. J.-C. Chambrion and J.-P. Sauvage, *Chem. Phys. Lett.*, 1991, **182**, 603-607.
20. M. N. Ackermann and L. V. Interrante, *Inorg. Chem.*, 1984, **23**, 3904-3911.
21. F. Barigletti, A. Juris, V. Balzani, P. Belser and A. Von Zelewsky, *Inorg. Chem.*, 1987, **26**, 4115-4119.
22. E. Amouyal, A. Homsí, J.-C. Chambrion and J.-P. Sauvage, *J. Chem. Soc.: Dalton Trans.*, 1990, 1841-1845.
23. J. Fees, W. Kaim, M. Moscherosch, W. Matheis, J. Klima, M. Krejčík and S. Zalis, *Inorg. Chem.*, 1993, **32**, 166-174.
24. E. J. C. Olson, D. Hu, A. Hörmann, A. M. Jonkman, M. R. Arkin, E. D. A. Stemp, J. K. Barton and P. F. Barbara, *J. Am. Chem. Soc.*, 1997, **119**, 11458-11467.
25. R. B. Nair, B. M. Cullum and C. J. Murphy, *Inorg. Chem.*, 1997, **36**, 962-965.
26. C. G. Coates, P. L. Callaghan, J. J. McGarvey, J. M. Kelly, P. E. Kruger and M. E. Higgins, *J. Raman. Spec.*, 2000, **31**, 283-288.
27. F. E. Poynton, J. P. Hall, P. M. Keane, C. Schwarz, I. V. Sazanovich, M. Towrie, T. Gunnlaugsson, C. J. Cardin, D. J. Cardin, S. J. Quinn, C. Long and J. M. Kelly, *Chem. Sci.*, 2016, **7**, 3075-3084.
28. P. M. Keane and J. M. Kelly, *Coord. Chem. Rev.*, 2018, **364**, 137-154.
29. A. W. McKinley, P. Lincoln and E. M. Tuite, *Coord. Chem. Rev.*, 2011, **255**, 2676-2692.
30. B. Önfelt, P. Lincoln, B. Nordén, J. S. Baskin and A. H. Zewail, *Proc. Nat. Acad. Sci.*, 2000, **97**, 5708-5713.
31. C. G. Coates, J. Olofsson, M. Coletti, J. J. McGarvey, B. Önfelt, P. Lincoln, B. Norden, E. Tuite, P. Matousek and A. W. Parker, *J. Phys. Chem. B*, 2001, **105**, 12653-12664.
32. J. Olofsson, B. Önfelt, P. Lincoln, B. Nordén, P. Matousek, A. W. Parker and E. Tuite, *J. Inorg. Biochem.*, 2002, **91**, 286-297.
33. M. K. Brennaman, J. H. Alstrum-Acevedo, C. N. Fleming, P. Jang, T. J. Meyer and J. M. Papanikolas, *J. Am. Chem. Soc.*, 2002, **124**, 15094-15098.

34. M. K. Brennaman, T. J. Meyer and J. M. Papanikolas, *J. Phys. Chem. A*, 2004, **108**, 9938-9944.
35. J. Van Houten and R. J. Watts, *J. Am. Chem. Soc.*, 1976, **98**, 4853-4858.
36. L. Wallace, D. C. Jackman, D. P. Rillema and J. W. Merkert, *Inorg. Chem.*, 1995, **34**, 5210-5214.
37. H. Uoyama, K. Goushi, K. Shizu, H. Nomura and C. Adachi, *Nature*, 2012, **492**, 234-238.
38. T. J. Penfold, F. B. Dias and A. P. Monkman, *Chem. Commun.*, 2018, **54**, 3926-3935.
39. Y. Zhang, T. S. Lee, J. M. Favale, D. C. Leary, J. L. Petersen, G. D. Scholes, F. N. Castellano and C. Milsmann, *Nat. Chem.*, 2020, **12**, 345-352.
40. F. N. Castellano, *Acc. Chem. Res.*, 2015, **48**, 828-839.
41. A. J. Howarth, M. B. Majewski and M. O. Wolf, *Coord. Chem. Rev.*, 2015, **282-283**, 139-149.
42. N. D. McClenaghan, Y. Leydet, B. Maubert, M. T. Indelli and S. Campagna, *Coord. Chem. Rev.*, 2005, **249**, 1336-1350.
43. C. B. Larsen, G. A. Farrow, L. D. Smith, M. V. Appleby, D. Chekulaev, J. A. Weinstein and O. S. Wenger, *Inorg. Chem.*, 2020, **59**, 10430-10438.
44. M. Borgström, O. Johansson, R. Lomoth, H. B. Baudin, S. Wallin, L. Sun, B. Åkermark and L. Hammarström, *Inorg. Chem.*, 2003, **42**, 5173-5184.
45. J. Hankache and O. S. Wenger, *Phys. Chem. Chem. Phys.*, 2012, **14**, 2685-2692.
46. G. Hager and G. Crosby, *J. Am. Chem. Soc.*, 1975, **97**, 7031-7037.
47. J. V. Caspar and T. J. Meyer, *J. Am. Chem. Soc.*, 1983, **105**, 5583-5590.
48. B. Durham, J. V. Caspar, J. K. Nagle and T. J. Meyer, *J. Am. Chem. Soc.*, 1982, **104**, 4803-4810.
49. R. S. Lumpkin, E. M. Kober, L. A. Worl, Z. Murtaza and T. J. Meyer, *J. Phys. Chem.*, 1990, **94**, 239-243.
50. W. R. Cherry and L. J. Henderson Jr, *Inorg. Chem.*, 1984, **23**, 983-986.
51. W. F. Wacholtz, R. A. Auerbach and R. H. Schmehl, *Inorg. Chem.*, 1986, **25**, 227-234.
52. R. W. Harrigan and G. A. Crosby, *J. Chem. Phys.*, 1973, **59**, 3468-3476.
53. E. M. Kober and T. J. Meyer, *Inorg. Chem.*, 1984, **23**, 3877-3886.
54. R. A. Marcus and N. Sutin, *Biochim. Biophys. Acta, Bioenerg.*, 1985, **811**, 265-322.
55. P. F. Barbara, T. J. Meyer and M. A. Ratner, *J. Phys. Chem.*, 1996, **100**, 13148-13168.
56. E. J. Piechota, R. N. Sampaio, L. Troian-Gautier, A. B. Maurer, C. P. Berlinguette and G. J. Meyer, *J. Phys. Chem. C*, 2019, **123**, 3416-3425.
57. G. A. Neyhart, C. J. Timpson, W. D. Bates and T. J. Meyer, *J. Am. Chem. Soc.*, 1996, **118**, 3730-3737.
58. H. Heitele, F. Pöllinger, S. Weeren and M. E. Michel-Beyerle, *Chem. Phys. Lett.*, 1990, **168**, 598-604.
59. D. V. Matyushov and R. Schmid, *Chem. Phys. Lett.*, 1994, **220**, 359-364.
60. J. T. Hupp and M. J. Weaver, *Inorg. Chem.*, 1984, **23**, 3639-3644.
61. R. Marcus and N. Sutin, *Inorg. Chem.*, 1975, **14**, 213-216.
62. J. R. Lakowicz, *Principles of fluorescence spectroscopy*, Kluwer Academic/Plenum, 1999.
63. H. Oevering, M. N. Paddon-Row, M. Heppener, A. M. Oliver, E. Cotsaris, J. W. Verhoeven and N. S. Hush, *J. Am. Chem. Soc.*, 1987, **109**, 3258-3269.
64. A. Weller, *Zeit. Phys. Chem.*, 1982, **133**, 93-98.
65. C. Reichardt, *Chem. Rev.*, 1994, **94**, 2319-2358.
66. J. Hankache, M. Niemi, H. Lemmetyinen and O. S. Wenger, *J. Phys. Chem. A*, 2012, **116**, 8159-8168.
67. G. G. Gurzadyan and S. Steenken, *Chem. Eur. J.*, 2001, **7**, 1808-1815.